

PPM1D activity promotes cellular transformation by preventing senescence and cell death

Miroslav Stoyanov, Andra S. Martinikova, Katerina Matejkova, Klara Horackova, Petra Zemankova, Kamila Burdova, Zuzana Zemanova, Petra Kleiblova, Zdenek Kleibl, Libor Macurek

Supplementary Figures S1-S11

Suppl. Fig. S1. Validation of a mouse monoclonal antibody to PPM1D

Suppl. Fig. S2. Activation of cGAS pathway in cells with truncated PPM1D after exposure to IR

Suppl. Fig. S3. Karyotyping of the transformed RPE-PPM1D-T2-SA cells

Suppl. Fig. S4. Volcano plots from transcriptomic analysis of the transformed RPE-PPM1D-T2 cells

Suppl. Fig. S5. Clustering analysis of the parental and transformed RPE-PPM1D-T2 cells

Suppl. Fig. S6. Transformed RPE-PPM1D-T2-SA clones remain p53 proficient

Suppl. Fig. S7. Similarity metrics heat maps for the transformed RPE-PPM1D-T2-SA clones

Suppl. Fig. S8. Treemap plots for the transformed RPE-PPM1D-T2-SA clones

Suppl. Fig. S9. Significantly enriched parental GO:BP terms in individual RPE-PPM1D-T2-SA clones

Suppl. Fig. S10. Truncated PPM1D promotes override of OIS in cells expressing active RAS

Suppl. Fig. S11. Senescence induced by RAS is p53 dependent

Legend to Supplementary Tables 1-3

Suppl. Table 1. Expression profiling of the transformed RPE-PPM1D-T2-SA clones

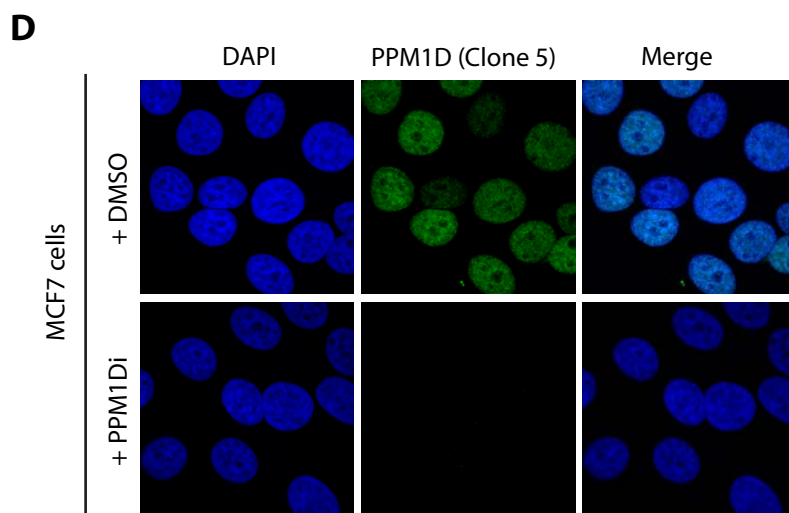
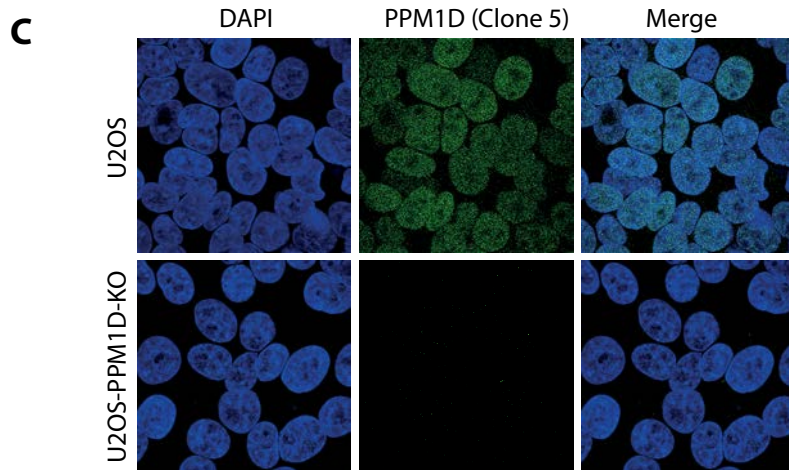
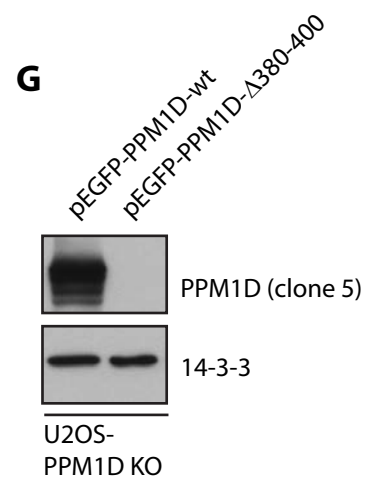
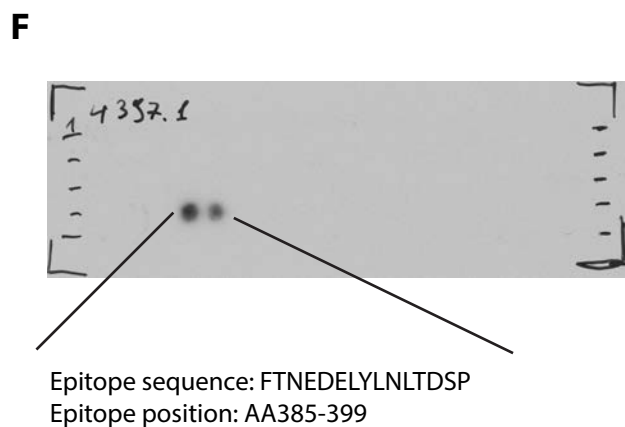
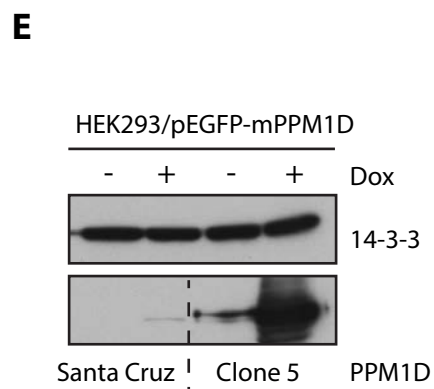
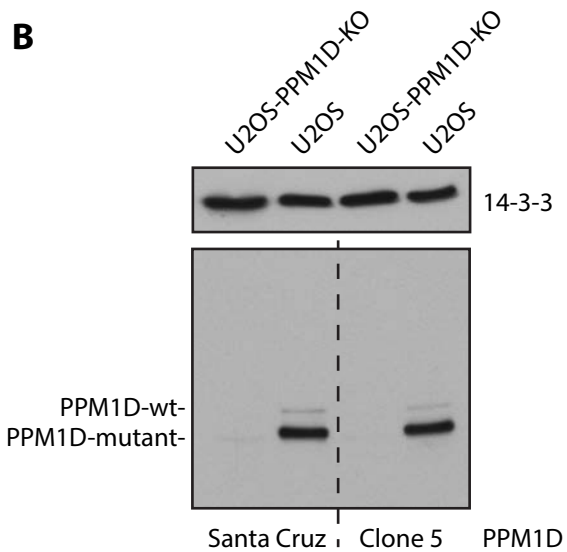
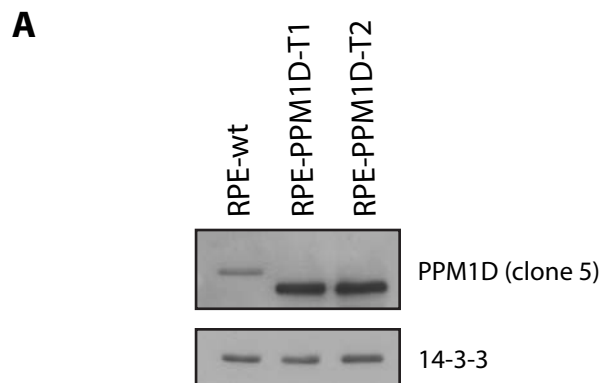
Suppl. Table 2. Genotypes of the transformed RPE-PPM1D-T2-SA clones

Suppl. Table 3. GSEA analysis comparing individual RPE-PPM1D-T2-SA clones with parental cells

Suppl. Fig. S1. Validation of a mouse monoclonal antibody to PPM1D

A) Whole cell lysates from parental RPE, RPE-PPM1D-T1 and RPE-PPM1D-T2 cells were probed with the custom-made mouse monoclonal PPM1D (clone 5) antibody. **B)** Parental U2OS and U2OS-PPM1D-KO cells lacking PPM1D were probed with PPM1D (clone 5) antibody. Note that U2OS cells contain the wild type and mutant allele of *PPM1D* leading to expression of the full-length and C-terminally truncated PPM1D. **C)** Parental U2OS and U2OS-PPM1D-KO cells were fixed by PFA, stained with PPM1D (clone 5) antibody (2 µg/mL) and imaged by confocal microscopy. **D)** MCF7 cells treated or not with PPM1Di were fixed by PFA, stained with PPM1D (clone 5) antibody and imaged by confocal microscopy. Note that treatment with PPM1Di leads to strong reduction of PPM1D levels in cells, confirming the specificity of the observed signal. **E)** HEK293 cells were transfected with plasmid expressing the mouse PPM1D and reactivity of the commercial PPM1D (Santa Cruz) and custom made PPM1D (clone 5) antibodies was compared by immunoblotting. **F)** Epitope mapping of the PPM1D (clone 5) antibody using PepSpot peptides immobilized on nitrocellulose membrane. The epitope was mapped to aa 385-399 (FTNEDELYLNLTDSP) of human PPM1D. **G)** U2OS-PPM1D-KO cells were transfected with full length EGFP-PPM1D or mutant lacking AA380-400 and reactivity of PPM1D (clone 5) antibody was tested using immunoblotting.

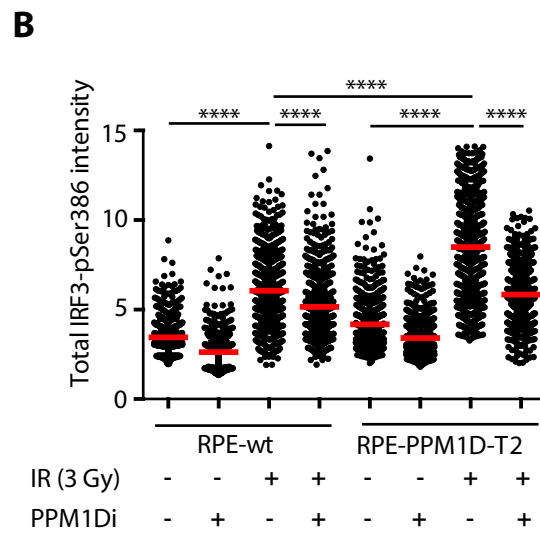
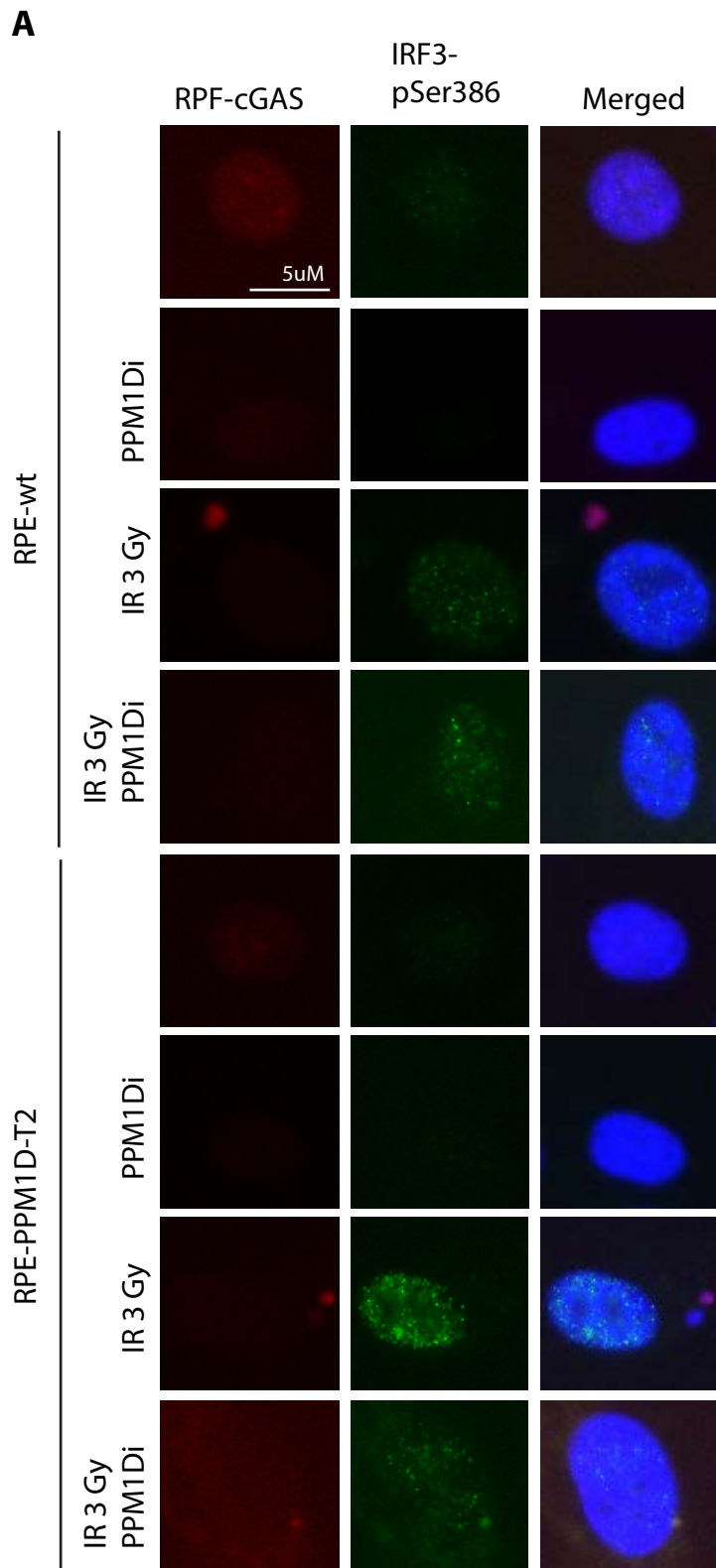
Supplementary Fig. 1



Suppl. Fig. S2. Activation of cGAS pathway in cells with truncated PPM1D after exposure to IR

A) Parental RPE and RPE-PPM1D-T2 stably transfected with RFP-cGAS were mock treated or irradiated (3 Gy) in the presence or absence of PPM1Di, fixed after 48 h and probed for IRF3-pS386 by ScanR microscopy. Representative images are shown. **B)** Quantification of IRF3-pS386 signal from A. Each dot represents a single cell. Red bar indicates median. Statistical significance was evaluated by Student's t-test (***) $p \leq 0.001$).

Supplementary Fig. 2

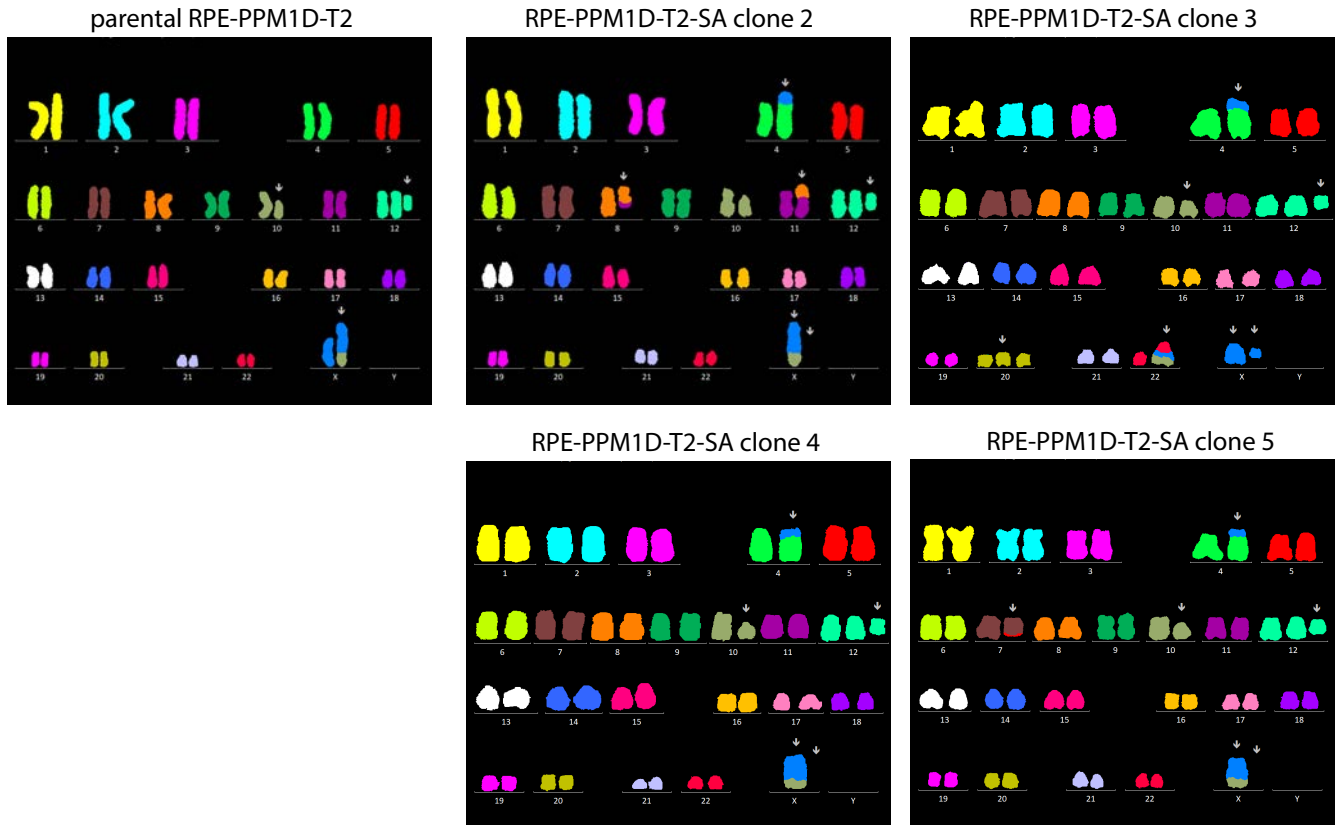


Suppl. Fig. S3. Karyotyping of the transformed RPE-PPM1D-T2-SA cells

A) Parental RPE-PPM1D-T2 cells and transformed RPE-PPM1D-T2-SA (clones 2 to 5) were arrested in mitosis, fixed and probed by M-FISH. **B)** Karyotyping of the parental RPE-PPM1D-T2 and all transformed RPE-PPM1D-T2-SA clones.

Suppl. Fig. S3

A

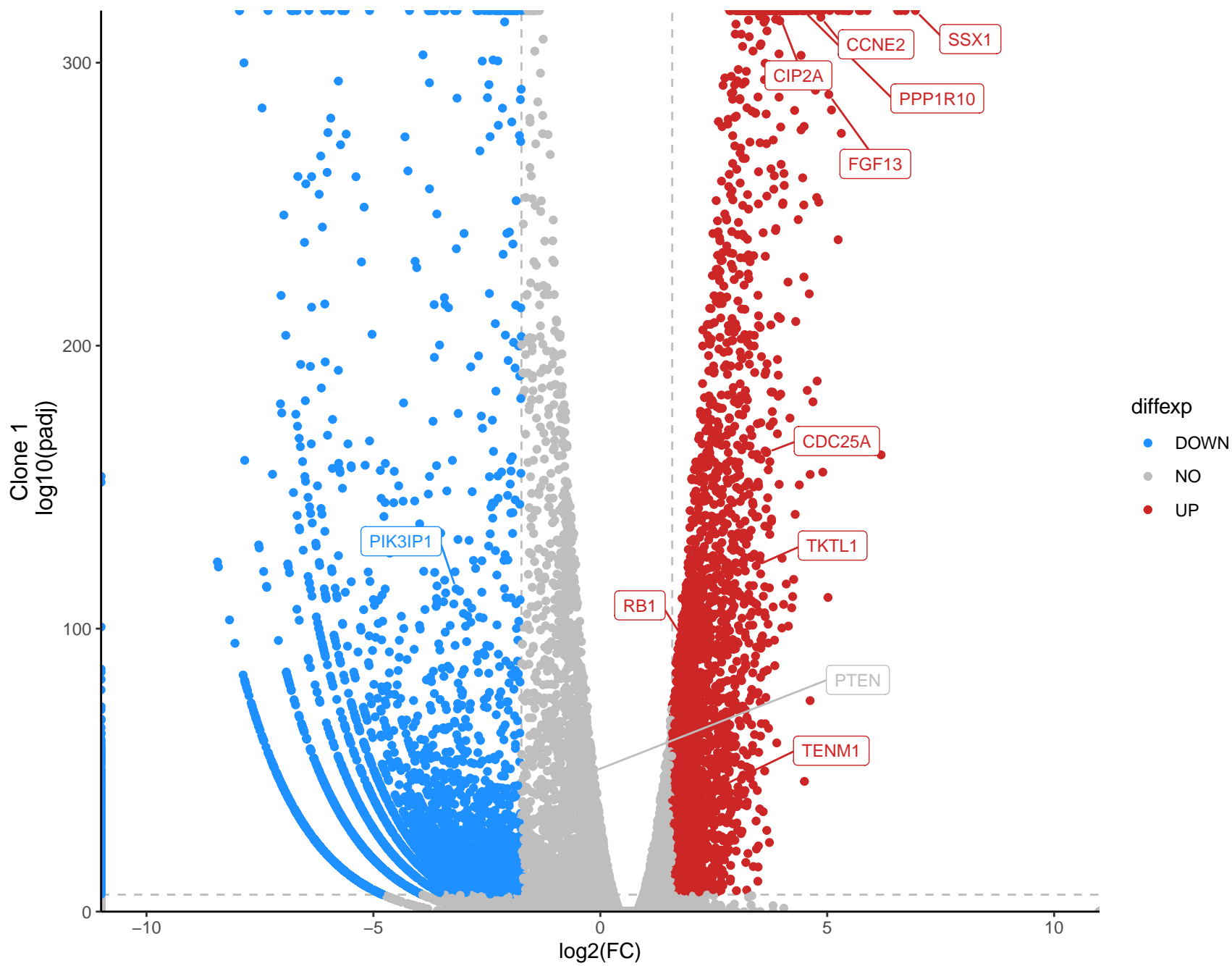


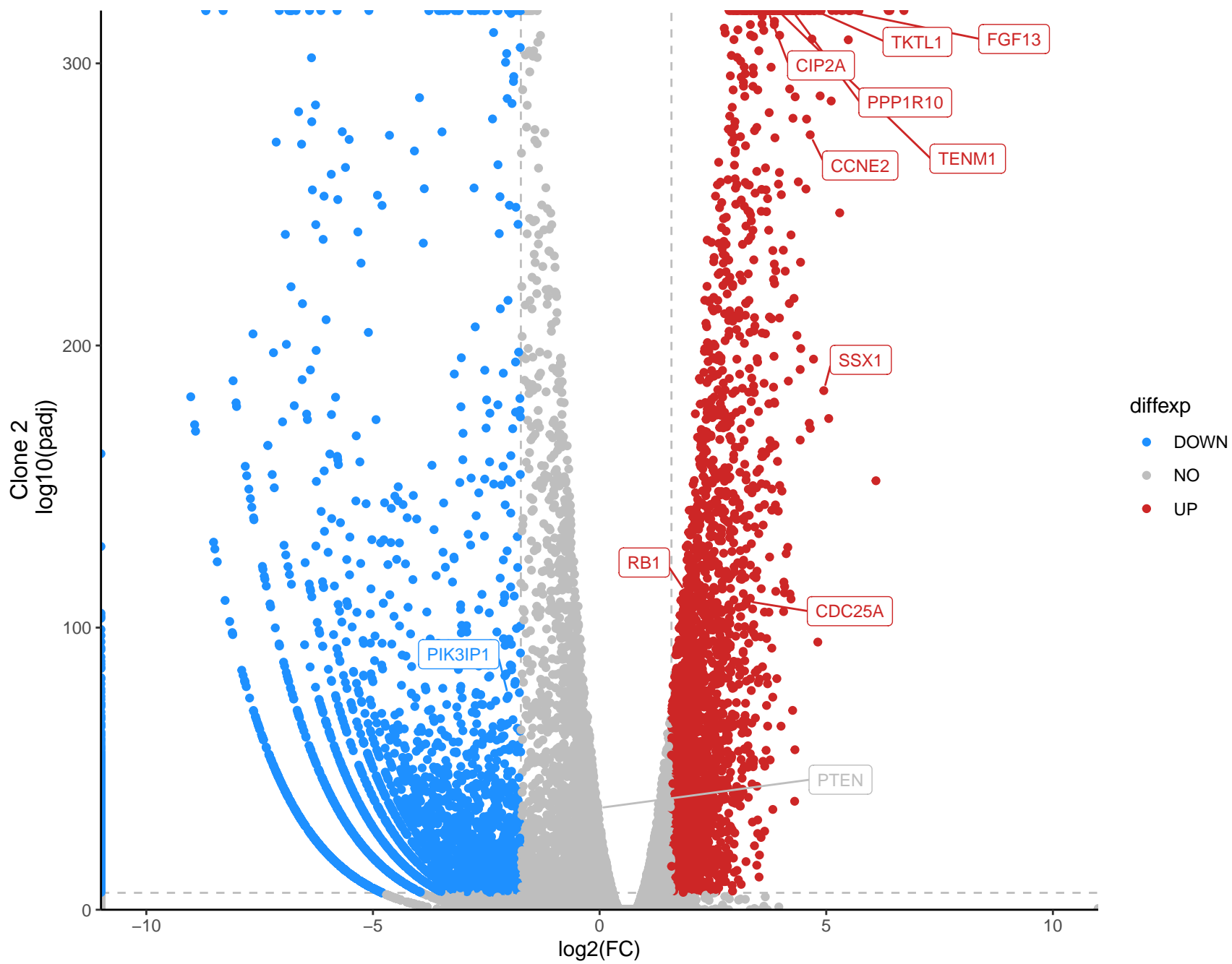
B

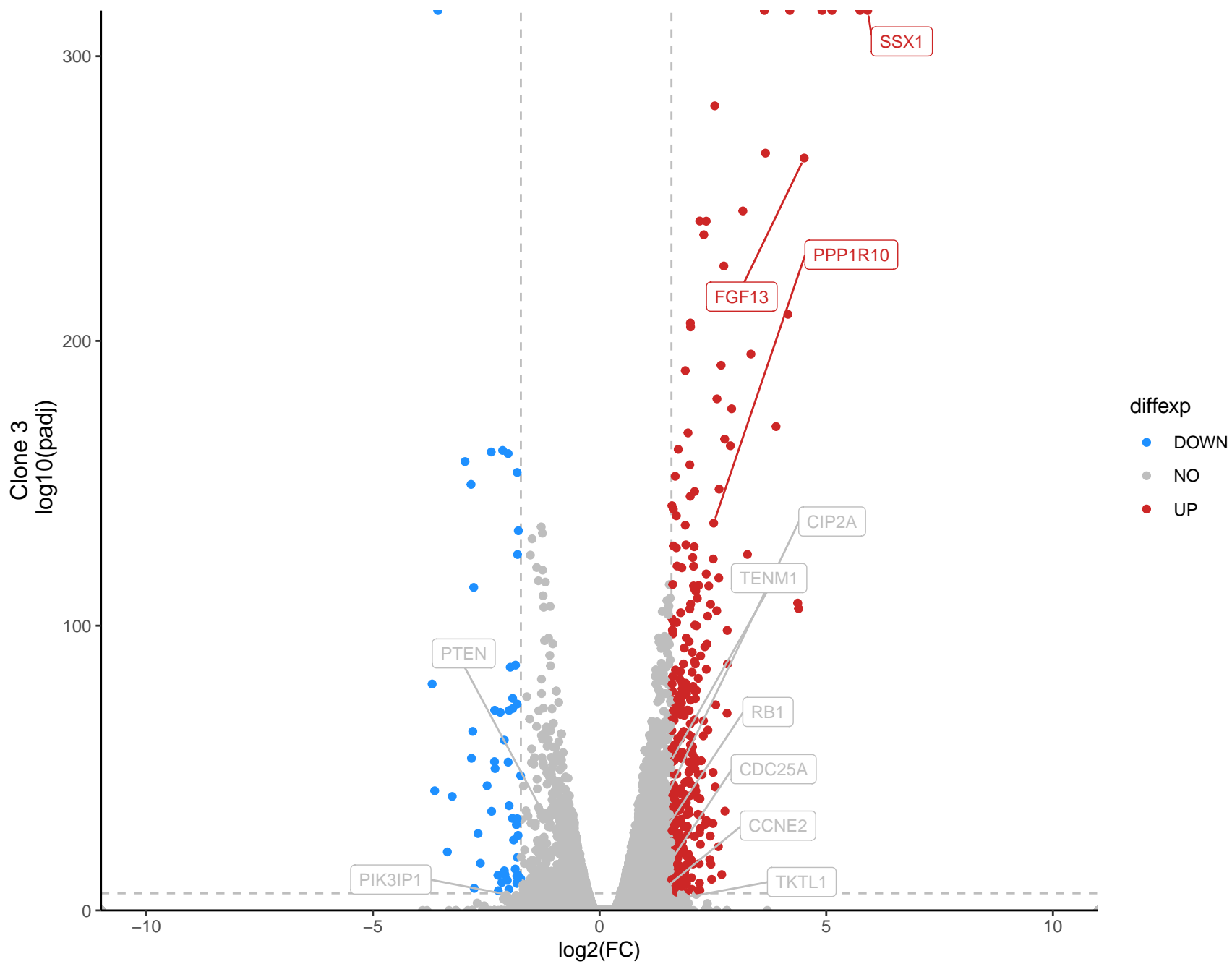
Cells	Karyotype
RPE-PPM1D-T2-SA clone 1	40~46,-X,der(X)t(X;7)(q13;q?),der(4)t(X;4)(?;p15),der(7)t(X;7)(q13;q11.23)t(X;10)(q28;q21.2),del(10)(p11.1),+i(12)(p10)[cp14]
RPE-PPM1D-T2-SA clone 2	40~46,-X,der(X)t(X;10)(q28;q21.2),der(4)t(X;4)(?;p15),t(8;11)(q13;p12),del(10)(p11.1),+i(12)(p10)[cp9]
RPE-PPM1D-T2-SA clone 3	42~48,del(X)(p11.1),r(X)(p11.1q13),der(4)t(X;4)(?;p15),del(10)(p11.1),+i(12)(p10),+20,der(22)t(X;22)(q13;q13)t(X;10)(q28;q21.2)[cp15]
RPE-PPM1D-T2-SA clone 4	40~46,-X,der(X)t(X;10)(q28;q21.2),der(4)t(X;4)(?;p15),del(10)(p11.1),+i(12)(p10)[cp24]
RPE-PPM1D-T2-SA clone 5	40~46,-X,der(X)t(X;10)(q28;q21.2),der(4)t(X;4)(?;p15),der(7)t(5;7)(?;q11.23),del(10)(p11.1),+i(12)(p10)[cp12]
RPE-PPM1D-T2-SA clone 6	41~46,-X,der(X)t(X;10)(q28;p11.2),t(2;11)(p13;p15),t(2;5)(p12;p11),der(4)t(X;4)(?;p15),ins(10;X)(p11.1;?),+i(12)(p10)[cp12]
parental RPE-PPM1D-T2 cells	33~47,X,der(X)t(X;10)(q28;q21.2),del(10)(p11.1),+i(12)(p10)[cp24]

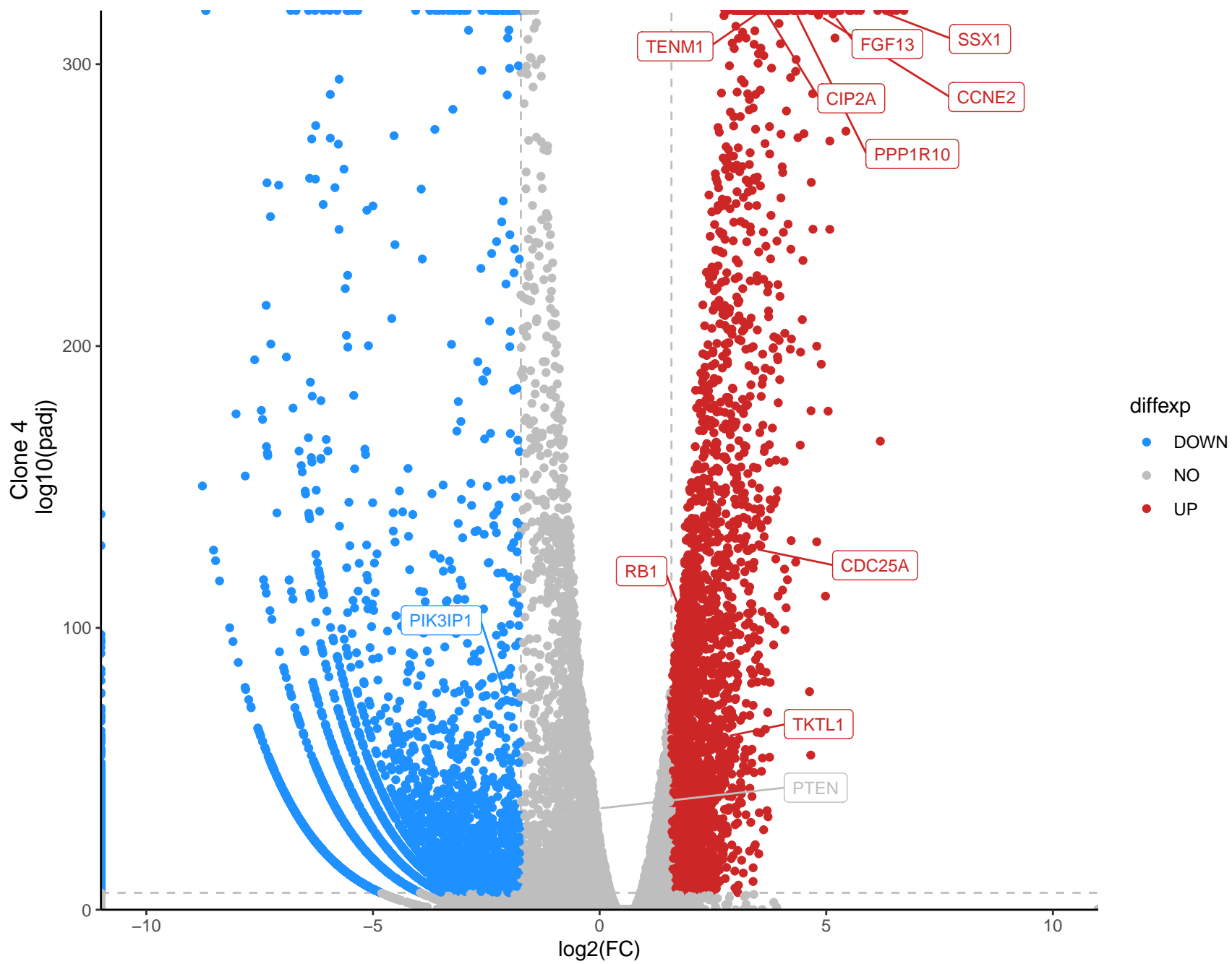
Suppl. Fig. S4. Volcano plots from transcriptomic analysis of the transformed RPE-PPM1D-T2 cells

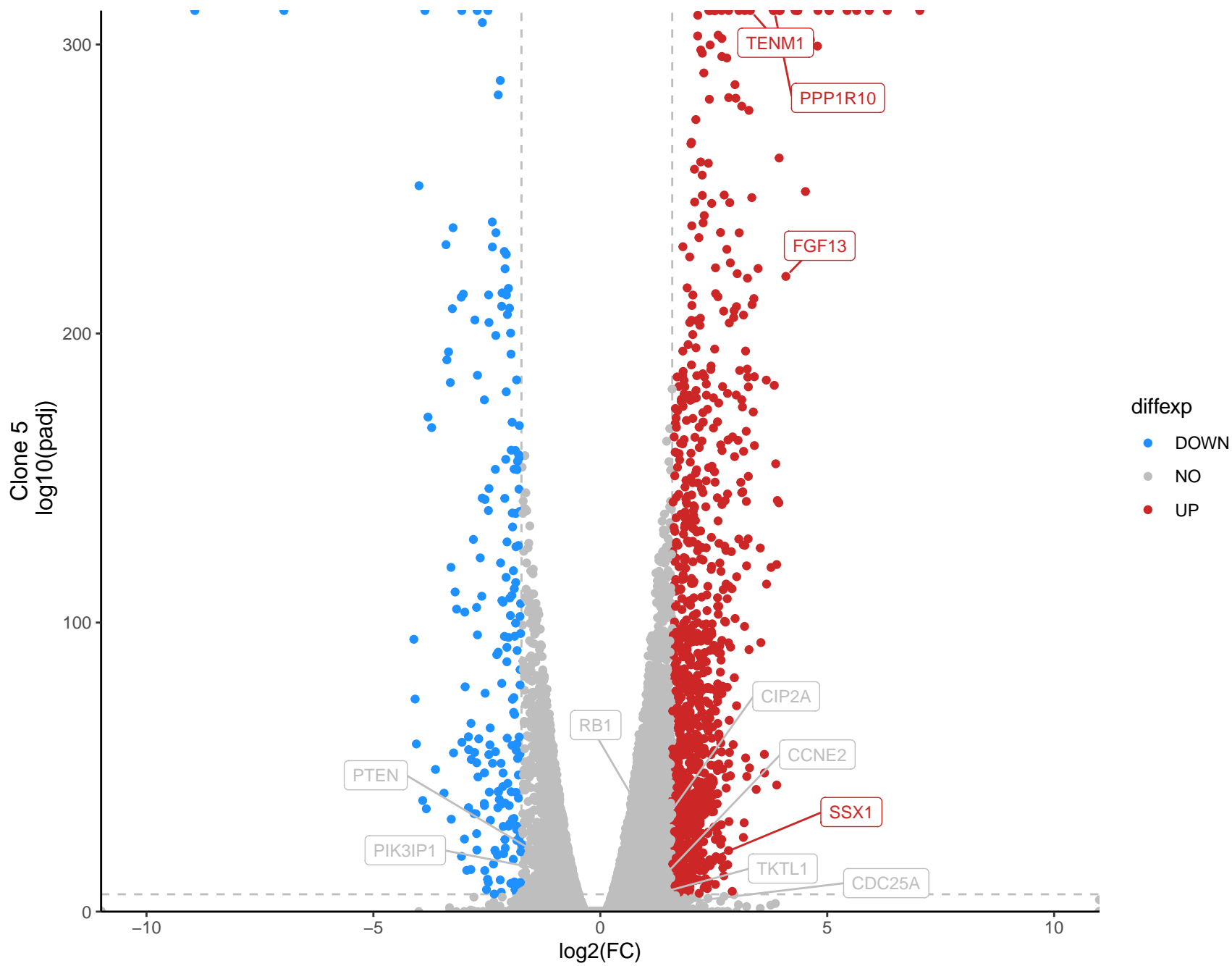
Volcano plots showing the differential expression of transcripts in the transformed RPE-PPM1D-T2-SA clones 1-6 compared to the parental RPE-PPM1D-T2 cells. Cut-off indicated by dashed lines was set to $p_{\text{adj}} < 0.000001$ and $FC > 3$ or $FC < 0.3$ for upregulated and downregulated genes, respectively. Significantly upregulated genes are shown in red, downregulated in blue.

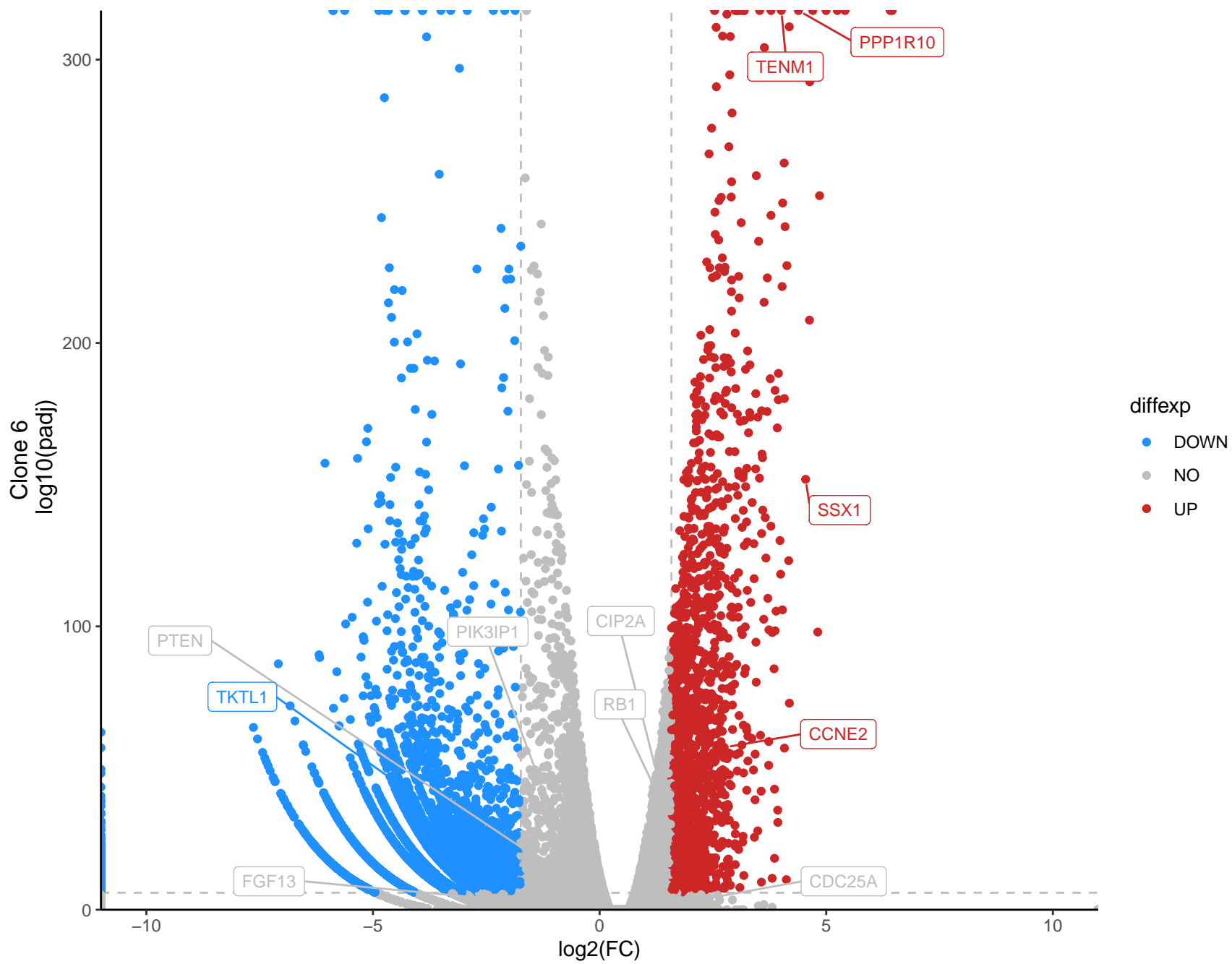








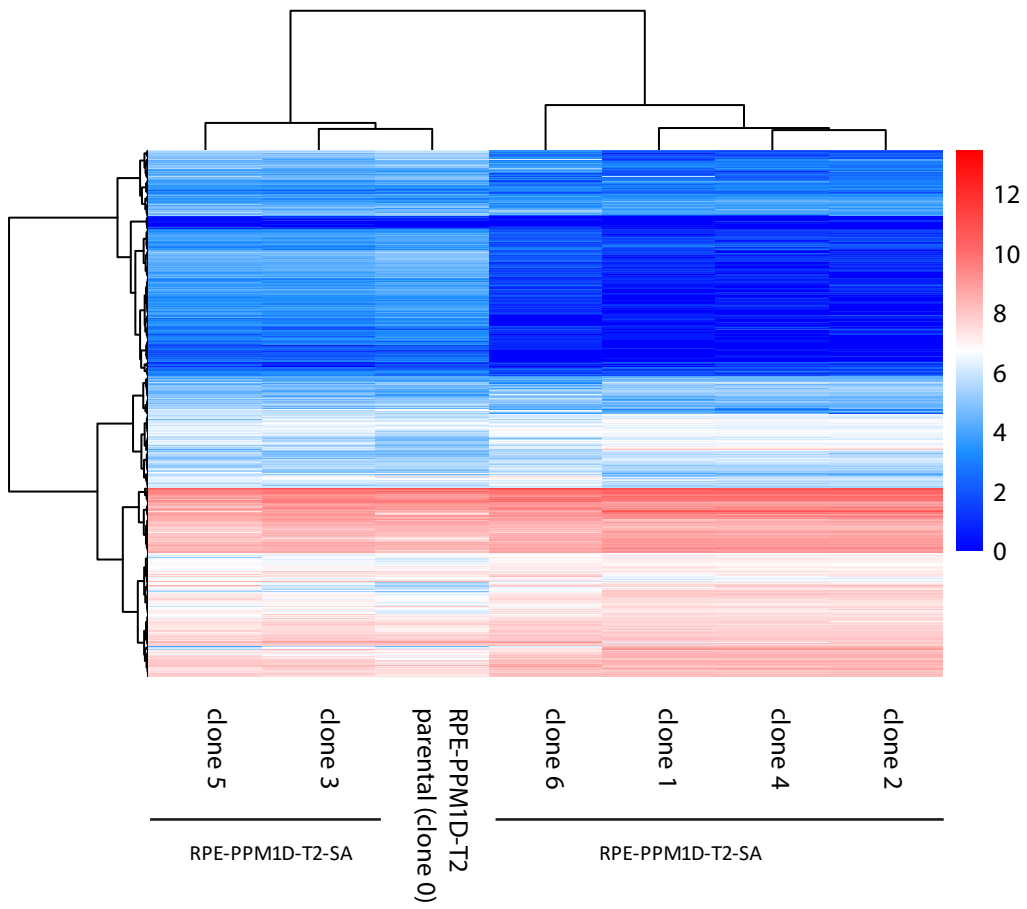




Suppl. Fig. S5. Clustering analysis of the parental and transformed RPE-PPM1D-T2 cells

Results of clustering analysis are depicted in heatmap with low expressed genes coloured blue and highly expressed genes coloured red. Logarithmized counts normalized with DESeq were used for the calculations. Ward.D2 algorithm was used as clustering method and Manhattan algorithm was used to measure distance. Transcription profiles of clones 1, 4 and 6 of the transformed RPE-PPM1D-T2 cells create one cluster, whereas clones 3 and 5 create another cluster with their transcription profiles more closely resembling the transcription profile of the parental RPE-PPM1D-T2 cells (depicted as clone 0).

Supplementary Fig. S5.

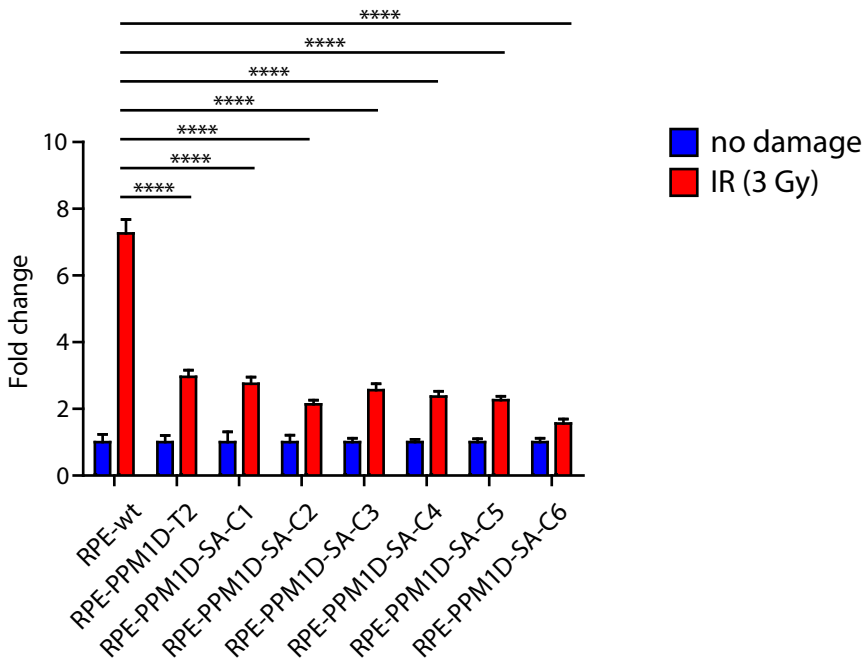


Suppl. Fig. S6. Transformed RPE-PPM1D-T2-SA clones remain p53 proficient

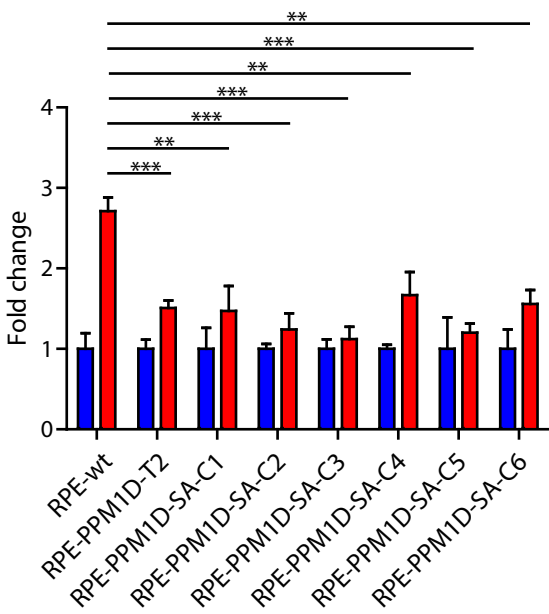
Parental RPE, RPE-PPM1D-T2 and transformed RPE-PPM1D-T2-SA cells were exposed or not to ionising radiation. Expression of indicated p53 target genes was evaluated by qPCR. Statistical significance was determined by t-test, error bars indicate SD, n=3.

Supplementary Fig. 6

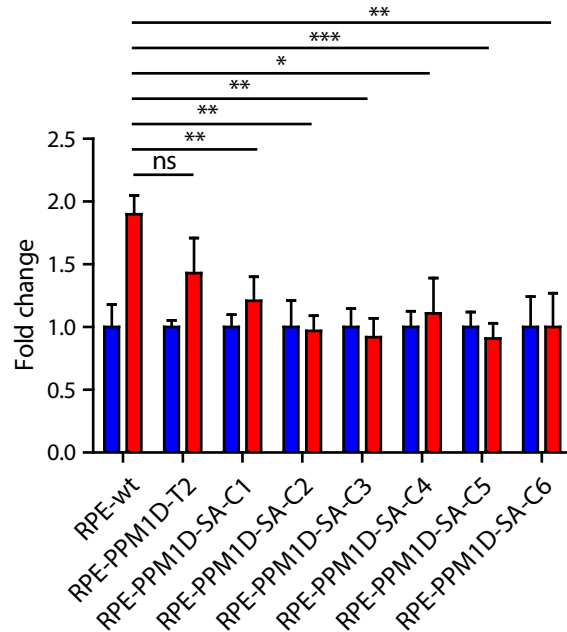
CDKN1A



NOXA



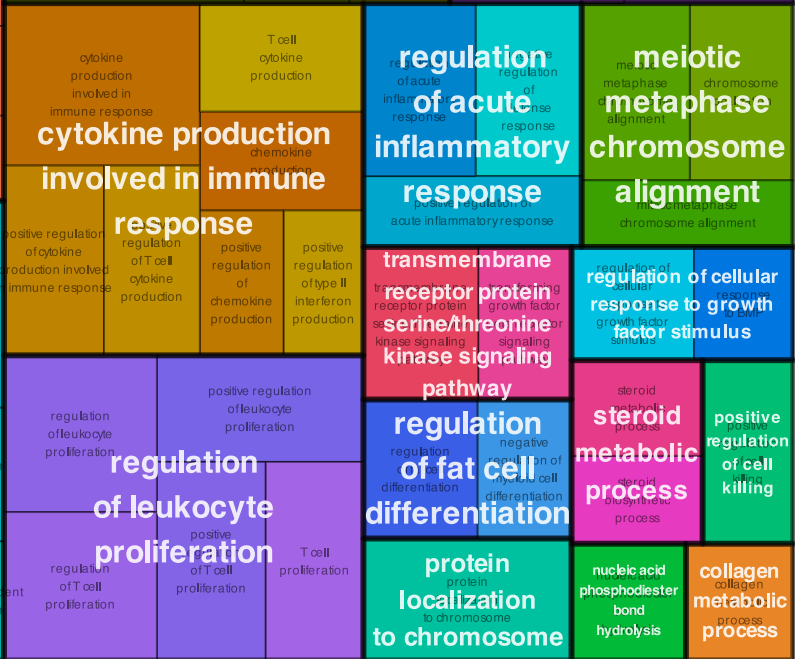
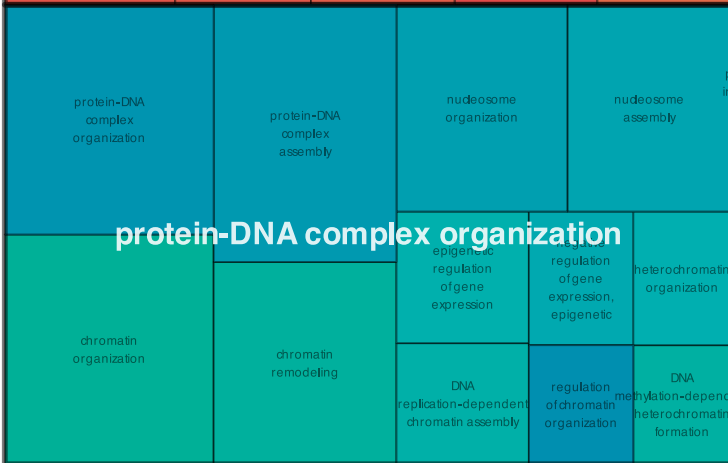
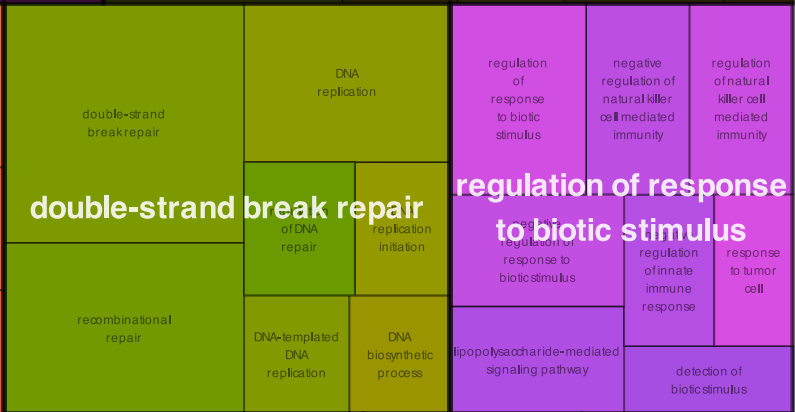
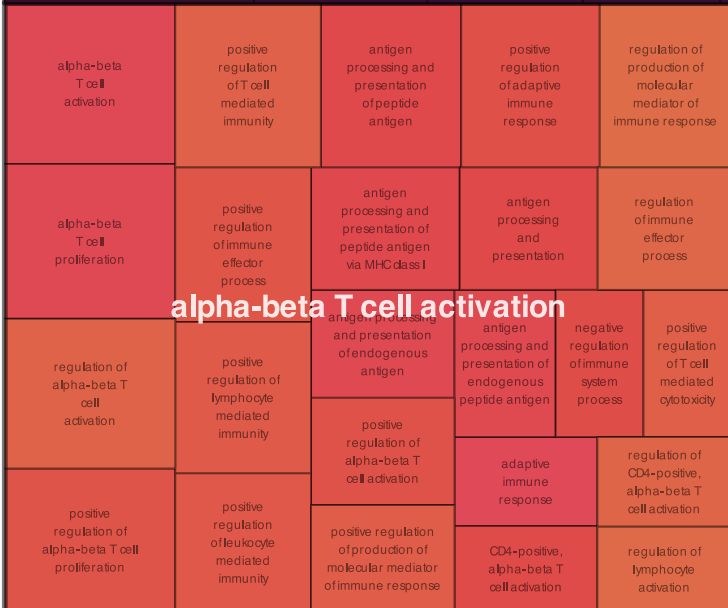
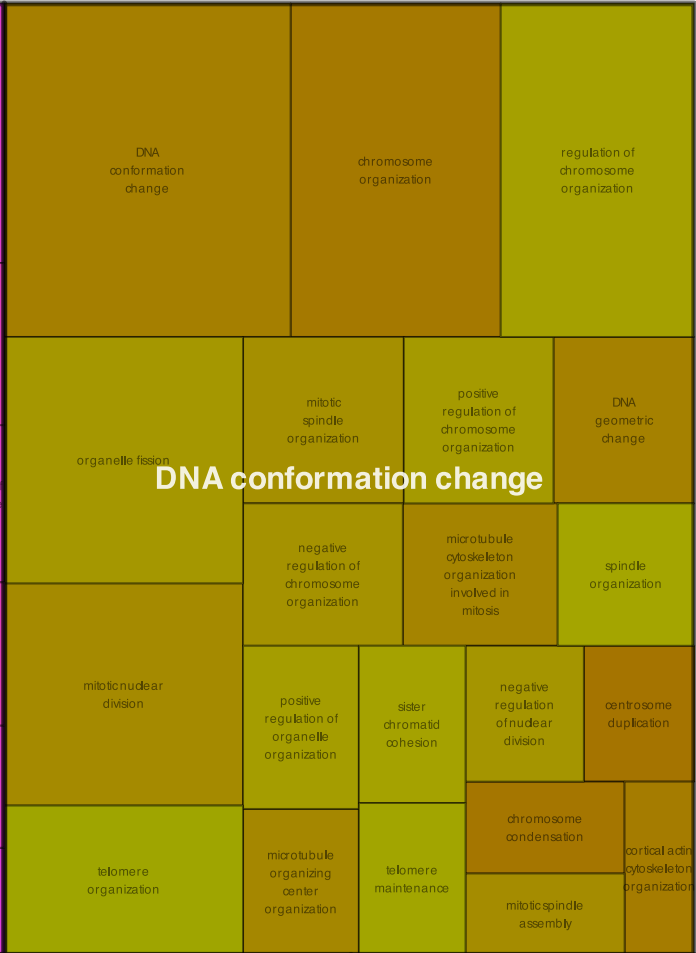
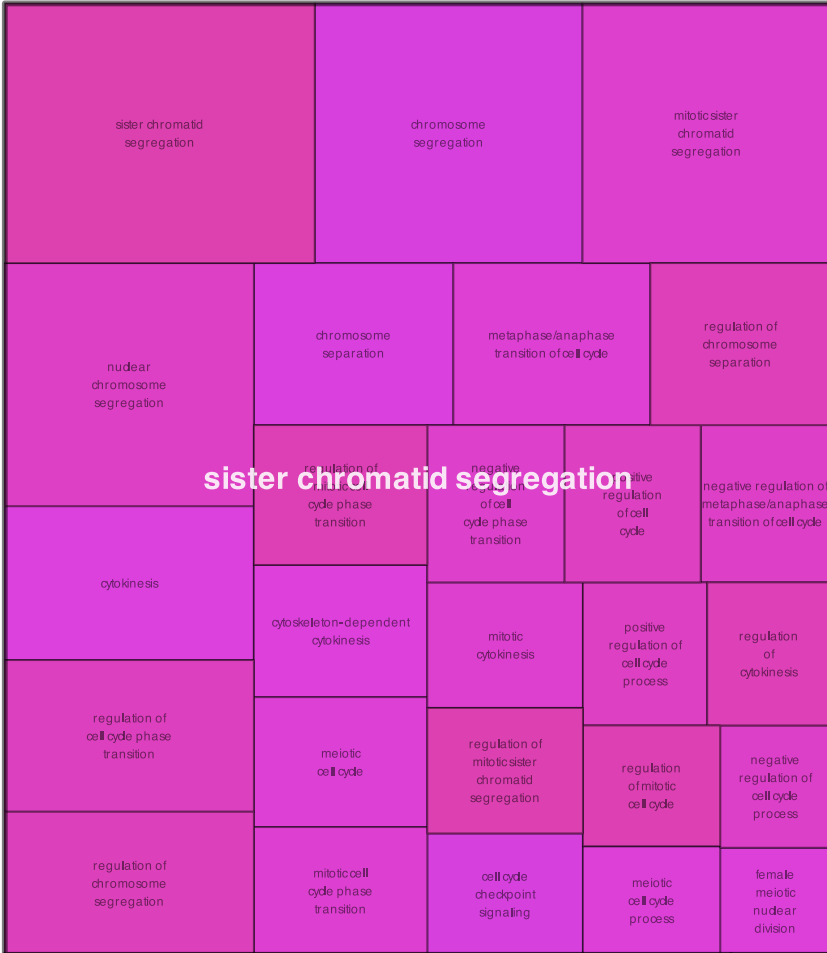
BAX



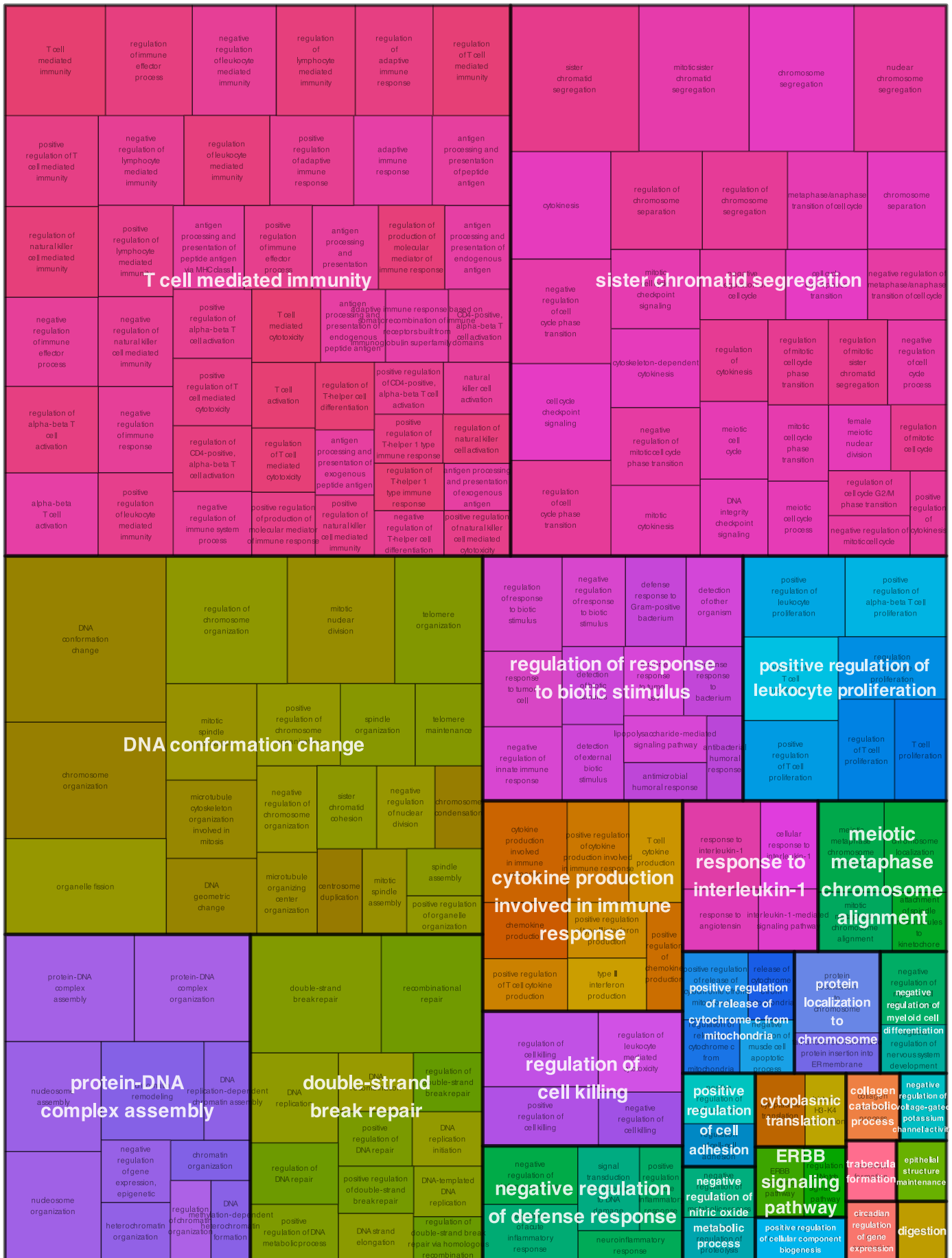
Suppl. Fig. S7. Similarity metrics heat maps for the transformed RPE-PPM1D-T2-SA clones

Similarity metrics heat maps generated by the rrvgo package aggregate related GO:BP (gene ontology: biological functions) terms enriched significantly from the GSEA analysis ($p_{adj} < 0.05$; Suppl Table 3). Clone #6 is not shown as it showed no significant GO:BP enrichment.

Suppl. Fig. S8. Treemap plots for the transformed RPE-PPM1D-T2-SA clones. Treemap plots generated by the rrvgo package express parent GO terms aggregating related GO:BP (gene ontology: biological functions) terms enriched significantly from the GSEA analysis ($p_{adj} < 0.05$; Suppl Table 3). Clone #6 is not shown as it showed no significant GO:BP enrichment.









regulation of leukocyte migration

G protein-coupled receptor signaling pathway, coupled to cyclic nucleotide second messenger

regulation of leukocyte migration

G protein-coupled receptor signaling pathway, coupled to cyclic nucleotide second messenger

positive regulation of leukocyte migration

neutrophil migration

neuropeptide signaling pathway

sensory perception of pain

keratinization

Suppl. Fig. S9. Significantly enriched parental GO:BP terms in individual RPE-PPM1D-T2-SA clones. Dots represent parental terms from GO:BP enriched in individual clones significantly ($p_{\text{adj}} < 0.05$; Suppl Table 3). The two largest collections of pathways including the DNA repair/replication processes and immune responses are highlighted in red and blue respectively.

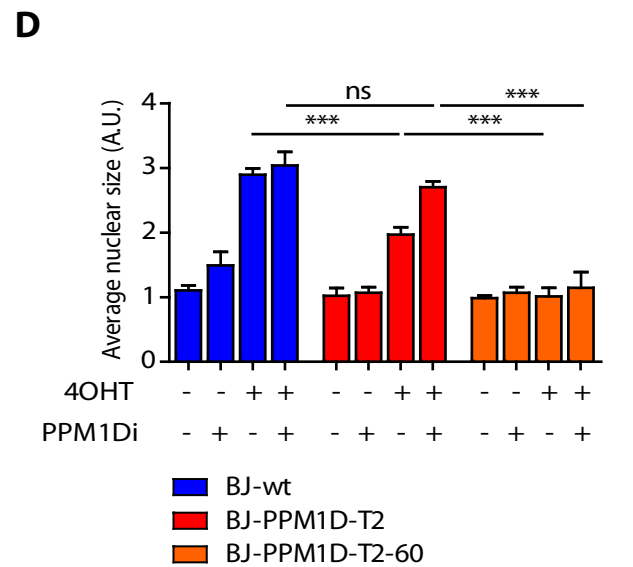
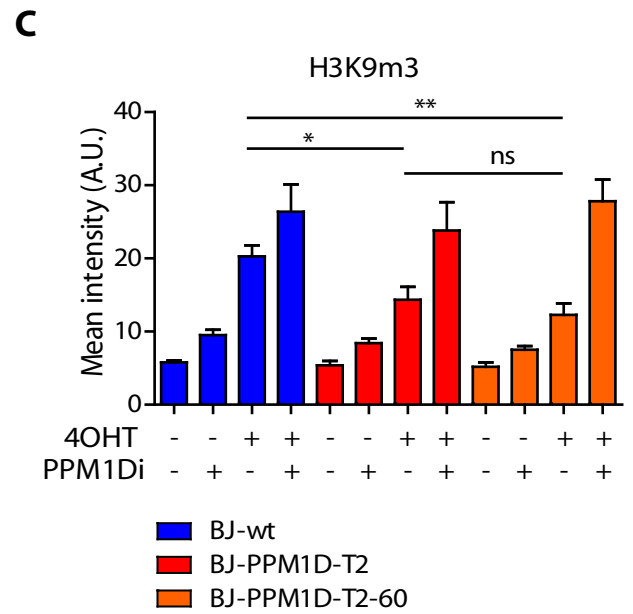
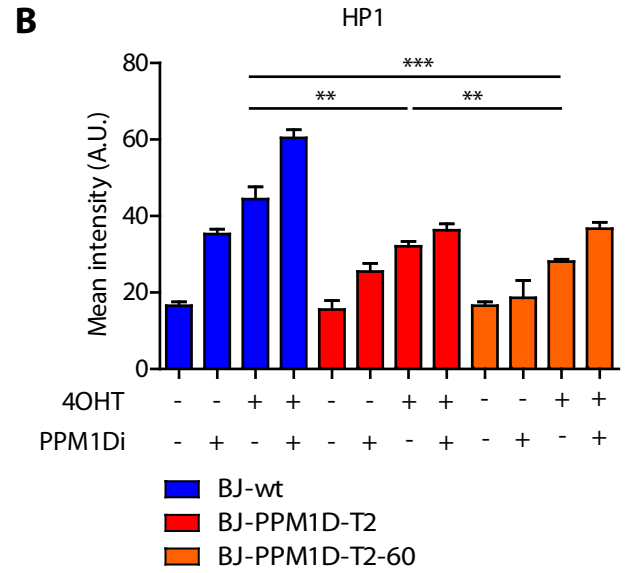
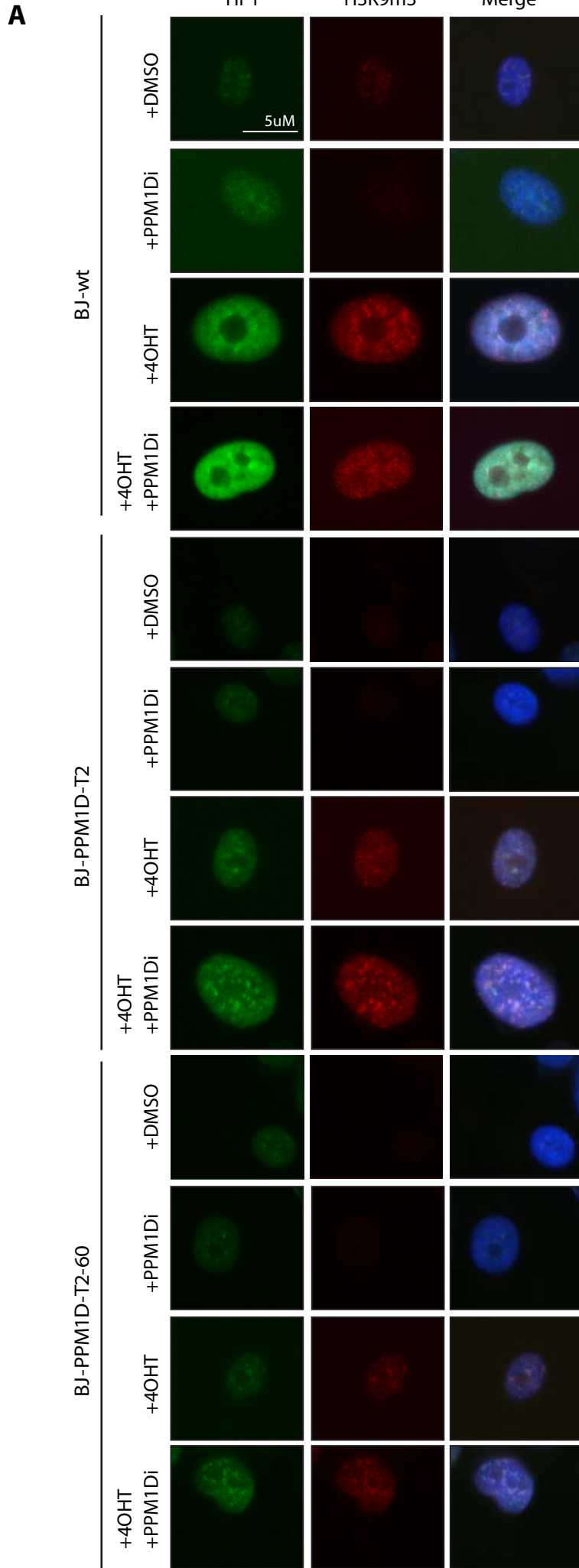
RPE-PPM1D-T2-SA

Parent GO term	RPE-PPM1D-T2-SA					
	Clone #1	Clone #2	Clone #4	Clone #3	Clone #5	Clone #6
Cytokine production involved in immune response	●	●	●			
Cytoplasmic translation		●	●	●		
DNA conformation change	●	●	●			
Double-strand break repair	●	●	●			
Meiotic metaphase chromosome alignment	●	●	●			
Protein localization to chromosome	●	●	●			
Regulation of response to biotic stimulus	●	●	●			
Sister chromatid segregation	●	●	●			
Epithelial structure maintenance		●	●			
Negative regulation of defense response		●	●			
Negative regulation of myeloid cell differentiation		●	●			
Positive regulation of leukocyte proliferation		●	●			
Protein localization to chromosome		●	●			
Protein-DNA complex assembly		●	●			
Regulation of cell killing		●	●			
Response to interleukin-1		●	●			
T cell mediated immunity		●	●			
Alpha-beta T cell activation	●					
Antimicrobial humoral immune response mediated by antimicrobial peptide				●		
Circadian regulation of gene expression			●			
G protein-coupled receptor signaling pathway					●	
Collagen catabolic process			●			
Collagen metabolic process	●					
Digestion			●			
Detection of chemical stimulus involved in sensory perception of taste				●		
ERBB signaling pathway			●			
Keratinization					●	
Leukocyte cell-cell adhesion		●				
Nucleic acid phosphodiester bond hydrolysis	●					
Negative regulation of lipid catabolic process		●				
Negative regulation of nitric oxide metabolic process			●			
Negative regulation of voltage-gated potassium channel activity			●			
Positive regulation of cell killing	●					
Positive regulation of cell adhesion			●			
Positive regulation of histone H3-K4 methylation		●				
Positive regulation of release of cytochrome c from mitochondria			●			
Protein-DNA complex organization	●					
Regulation of acute inflammatory response	●					
Regulation of cellular response to growth factor stimulus	●					
Regulation of fat cell differentiation	●					
Regulation of leukocyte migration					●	
Regulation of leukocyte proliferation	●					
Regulation of neurotrophin TRK receptor signaling pathway				●		
Sensory perception of pain					●	
Steroid metabolic process	●					
Transmembrane receptor protein serine/threonine kinase signaling pathway	●					
T-helper 17 cell differentiation				●		
Trabecula formation			●			

Suppl. Fig. S10. Truncated PPM1D promotes override of OIS in cells expressing active RAS

A) Parental BJ-hTert-HRASV12^{ER-TAM}, BJ-hTert-HRASV12^{ER-TAM}-PPM1D-T2, and BJ-hTert-HRASV12^{ER-TAM}-PPM1D-T2-60 cells that survived 2-months of HRASV12 expression were treated with combinations of 4OHT and PPM1D inhibitor for 20 days as indicated, fixed and stained for HP1, Histone H3K9me3 and DAPI and analyzed by ScanR microscopy. Representative images from three independent repeats are shown. Bar indicates 5 μ m. **B)** Quantification of the mean nuclear intensity of HP1 in BJ cells from A. **C)** Quantification of the mean nuclear intensity of Histone H3K9me3 in BJ cells from A. **D)** Quantification of the average nuclear size of BJ cells from A.

Supplementary Fig. S10

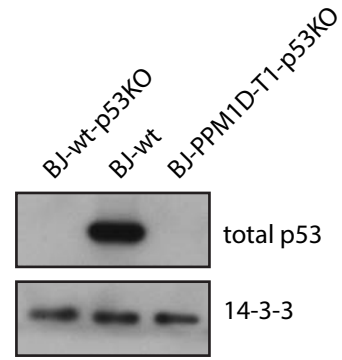
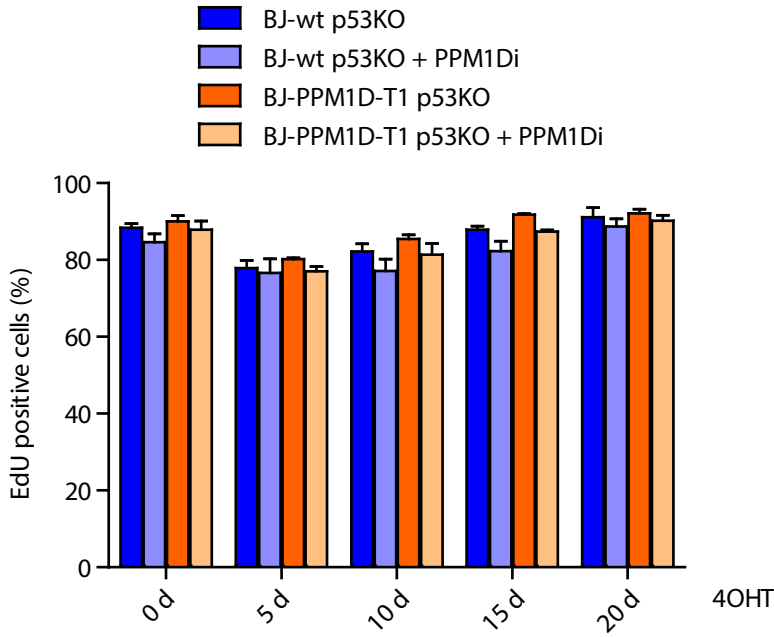


Suppl. Fig. S11. Senescence induced by RAS is p53 dependent

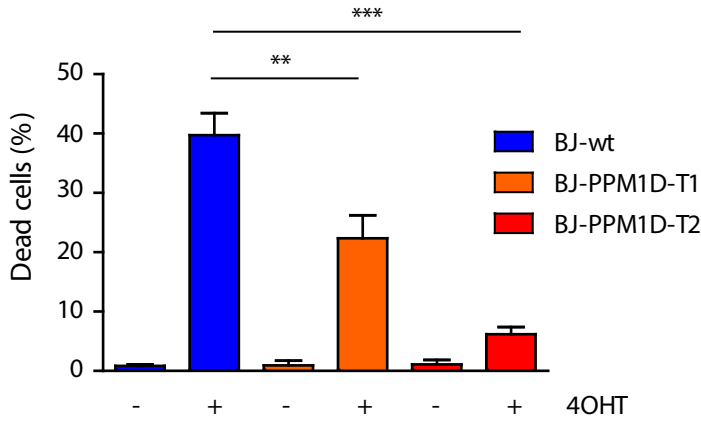
A) BJ-hTert-HRASV12^{ER-TAM}-TP53KO and BJ-hTert-HRASV12^{ER-TAM}-PPM1D-T1-TP53KO cells were cultivated in the presence of 4OHT and/or PPM1Di as indicated for 20 d. Cells were incubated with EdU 24 h prior fixation at indicated time intervals and EdU was labelled by CLICK-IT reaction. Fraction of EdU positive cells was analysed using FACS. The right panel shows immunoblotting analysis of p53 levels in BJ-hTert-HRASV12^{ER-TAM}, BJ-hTert-HRASV12^{ER-TAM}-TP53KO and BJ-hTert-HRASV12^{ER-TAM}-PPM1D-T1-TP53KO cells. **B)** BJ-hTert-HRASV12^{ER-TAM}, BJ-hTert-HRASV12^{ER-TAM}-PPM1D-T1 and -T2 cells were induced or not with 4OHT for 5 days. Cells were labelled by propidium iodide and DAPI and fraction of dead cells was determined by flow cytometry. **C)** mRNA was extracted from cells treated as in B and expression of *CDKN1A*, *NOXA* and *BAX* was determined by qPCR. Statistical significance was determined by t-test, error bars indicate SD, n=3. **D)** Fraction of cells incorporating EdU was determined after 60 days of 4OHT treatment of BJ-RAS-PPM1D-T1 and BJ-RAS-PPM1D-T2 cells by flow cytometry. **E)** Parental BJ-hTert-HRASV12^{ER-TAM}, BJ-hTert-HRASV12^{ER-TAM}-PPM1D-T2, BJ-hTert-HRASV12^{ER-TAM}-PPM1D-T1-60 and BJ-hTert-HRASV12^{ER-TAM}-PPM1D-T2-60 cells that managed to proliferate for 2 months of continuous 4OHT induction were collected 6 h after exposure to a high dose of IR (5 Gy). The ability to induce p21 expression was evaluated by immunoblotting.

Supplementary Fig. 11

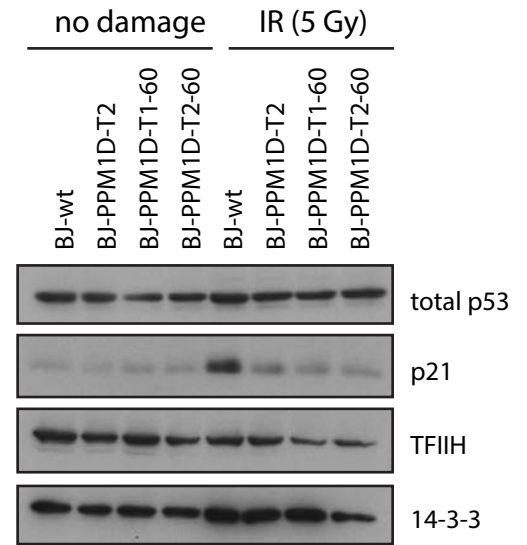
A



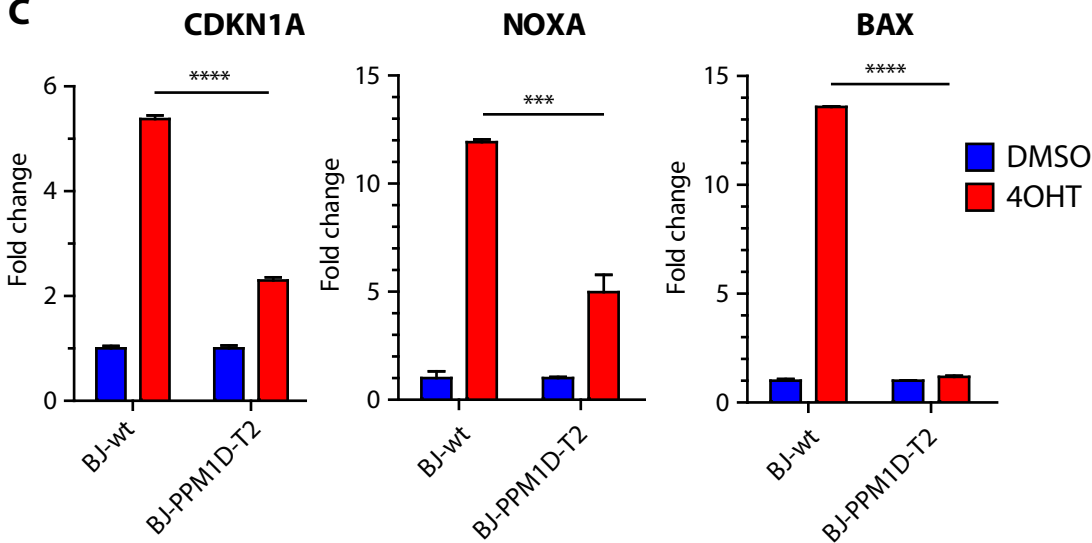
B



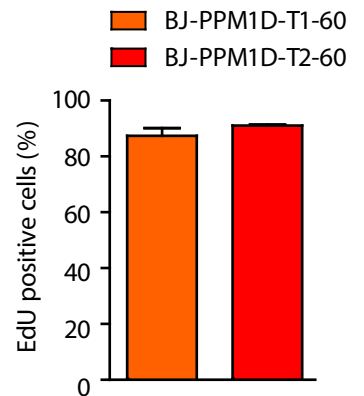
E



C



D



Suppl. Table 1. Expression profiling of the transformed RPE-PPM1D-T2-SA clones

RNA was isolated from nontransformed RPE-PPM1D-T2 cells and six transformed RPE-PPM1D-T2-SA clones. Sequencing libraries were prepared using RNA HyperPrep Kit and were sequenced on the NovaSeq 6000 system with mean coverage >120. All parts of RNAseq data analysis were conducted in R and RNAseq read counts were normalized using R package DESeq2. Fold change (FC) and \log_2FC were calculated from normalized reads, nontransformed RPE-PPM1D-T2 cells were considered a reference. Significance of differential expression for each gene was evaluated by Fisher's t-test with simulated p-values and Holm's p-value correction for multiple comparisons.

Suppl. Table 2. Genotypes of the transformed RPE-PPM1D-T2-SA clones

Genomic DNA variants (rows) from whole exome sequencing detected in the parental RPE-PPM1D-T2 (clone 0) and transformed RPE-PPM1D-T2-SA clones 1-6. Description of columns: A. Chromosome localization. B-C. Coordinate start/end (HG19). C-D. Nucleotide reference (ref)/alternative (alt). F. Gene. G. Reference transcript (NCBI). H. Length of canonical protein (amino acids). I. Codon change. H. Affected exon (if exonic variant). L-S. Variant characteristics. T-AG. Variant found in parental (0) and subsequent (1-6) clones. First column indicates the zygosity (1=heterozygote; 2=homozygote; NA=variant is not present=wild-type), second column describe allelic fraction of an alternative variant (minor allele frequency). AH. Maximal alternative allele frequency (regardless of population-specific cohort in the gnomAD database). AI. Variant listed in OMIM database (0=no; 1=yes). A0 – characteristics of the variant in the ClinVar database (assessed in 2023-12-12).

Suppl. Table 3. GSEA analysis comparing individual RPE-PPM1D-T2-SA clones (#1-6) with RPE-PPM1D-T2 parental cells. The GSEA analysis included all datasets from the Human MSigDB Collections (<https://www.gsea-msigdb.org/gsea/msigdb/human/collections.jsp>) available in the org.Hs.eg.db R-

package (accessed 2024-06-24). The sheet “all” includes data from the analysis for all clones. The sheet “summary GSEA statistics” provides overview of analysed and significantly changed gene subsets.